1521-0111/94/2/862–875$35.00
MOLECULAR PHARMACOLOGY

https://doi.org/10.1124/mol.118.112045
Mol Pharmacol 94:862–875, August 2018

Novel Paradigms Governing β_1-Adrenergic Receptor Trafficking in Primary Adult Rat Cardiac Myocytes

Mohammed M. Nooh, Salvatore Mancarella, and Suleiman W. Bahouth

Departments of Pharmacology (M.M.N., S.W.B.) and Physiology (S.M.), The University of Tennessee Health Sciences Center, Memphis, Tennessee; and Department of Biochemistry, Faculty of Pharmacy Cairo University, Cairo, Egypt (M.M.N.)

Received February 2, 2018; accepted May 23, 2018

ABSTRACT

The β_1-adrenergic receptor (β_1-AR) is a major cardiac G protein-coupled receptor, which mediates cardiac actions of catecholamines and is involved in genesis and treatment of numerous cardiovascular disorders. In mammalian cells, catecholamines induce the internalization of the β_1-AR into endosomes and their removal promotes the recycling of the endosomal β_1-AR back to the plasma membrane; however, whether these redistributive processes occur in terminally differentiated cells is unknown. Compartmentalization of the β_1-AR in response to β-agonists and antagonists was determined by confocal microscopy in primary adult rat ventricular myocytes (ARVMs), which are terminally differentiated myocytes with unique structures such as transverse tubules (T-tubules) and contractile sarcomeres. In unstimulated ARVMs, the fluorescently labeled β_1-AR was expressed on the external membrane (the sarcolemma) of cardiomyocytes. Exposing ARVMs to isoproterenol redistributed surface β_1-ARs into small (~225–250 nm) regularly spaced internal punctate structures that overlapped with puncta stained by Di-8 ANEPPS, a membrane-impermeant T-tubule-specific dye. Replacing the β-agonist with the β-blocker alprenolol, induced the translocation of the wild-type β_1-AR from these punctate structures back to the plasma membrane. This step was dependent on two barcodes, namely, the type-1 PDZ binding motif and serine at position 312 of the β_1-AR, which is phosphorylated by a pool of cAMP-dependent protein kinases anchored at the type-1 PDZ of the β_1-AR. These data show that redistribution of the β_1-AR in ARVMs from internal structures back to the plasma membrane was mediated by a novel sorting mechanism, which might explain unique aspects of cardiac β_1-AR signaling under normal or pathologic conditions.

Introduction

Activation of cardiac β_1-adrenergic receptor (β_1-AR) and β_2-adrenergic receptor (β_2-AR) by synaptic or circulating catecholamines increases cardiac cAMP that in turn activates cAMP-dependent protein kinase (PKA), which mediates catecholamine-dependent changes in rate, force, and speed of myocardial contractions (Lefkowitz et al., 2000). The activity of cAMP is vectored to specific cellular regions by compartmentalized signaling scaffolds that target phosphodiesterases and A-kinase anchoring proteins (AKAPs) to specific end locations within the cell (Baillie, 2009; Ellisdon and Halls, 2016). Moreover, spatial distribution of β_1-AR and β_2-AR in cardiomyocytes might provide an additional regulatory mechanism for controlling cAMP production and action (Valentine and Haggie, 2011). For example, spatial redistribution of cardiac β_2-AR in heart failure was associated with altered compartmentalization of cAMP and its downstream signaling in the heart (Nikolaev et al., 2010).

Given the prominence of β_1-ARs in regulating physiologic and pathologic signaling of catecholamine in the heart, it is important to know their distribution within the various cellular compartments of quiescent and catecholamine-activated adult rat ventricular cardiomyocytes. The distribution of many G protein-coupled receptors (GPCRs) in mammalian cells is altered by exposing these cells to chronic high concentrations of a GPCR agonist, which promotes the sequestration of many GPCRs, including the β_1-AR from the membrane to intracellular endosomes (Ferguson et al., 1996; Lefkowitz, 1998; Li et al., 2013). The fate of GPCRs in endosomes is regulated by barcodes that mediate either their retention and subsequent degradation in endosomes or their sorting out of endosomes and redistribution back to the plasma membrane (Hanyaloglu and von Zastrow, 2008).

A major barcode that governs the fate of the agonist-internalized GPCRs in endosomes is a C-terminal type-1 PDZ binding motif (PBM) found in many recycling GPCRs, including the β_1-ARs (Romero et al., 2011). In some cases, post-translational modifications such as ubiquitination assist the PBM in regulating the fate of a given GPCR or override the effect of the PBM on redistribution (Shenoy et al., 2001; Marchese and Trejo, 2013). Unlike other GPCRs,

This work was supported by the National Institutes of Health [Grant HL-085848] and by Bridge Funding support from the Office of the Vice Chancellor of The University of Tennessee–Health Sciences Center [B-2015-8].
https://doi.org/10.1124/mol.118.112045.

ABBREVIATIONS: Ad, adenovirus; AKAP, A-kinase anchoring protein; ALP, alprenolol; ANOVA, analysis of variance; ARVM, adult rat ventricular myocyte; β-AR, β-adrenergic receptor; β_1-AR, β_1-adrenergic receptor; β_2-AR, β_2-adrenergic receptor; GPCR, G protein-coupled receptor; ISO, isoproterenol; mPKI, myristoylated cAMP-dependent protein kinase inhibitory peptide; PBM, type-1 PDZ binding motif; ΔPDZ, deleted type-1 PDZ binding motif; PKA, cAMP-dependent protein kinase A; Ser^{312}, serine at position 312; shRNA, short hairpin RNA; S312A, mutation of serine at position 312 to alanine; SNX27, sorting nexin-27; T-tubule, transverse tubule; WT, wild type.

translocation of the agonist-internalized β_1-AR from endosomes to the plasma membrane was dependent on two barcodes, the PBM and a PKA-substrate serine at position 312 (Ser^{312}) in the third intracellular loop of the β_1-AR. Inactivation of these barcodes did not affect β-agonist-mediated translocation of the β_1-AR to endosomes, but inhibited β_1-AR redistribution from endosomes to the plasma membrane of mammalian cells, including cardiomyocytes prepared from neonatal rodents (Gardner et al., 2004; Li et al., 2013; Nooh and Bahouth, 2017).

In addition to barcodes, several GPCR accessory proteins were implicated in the regulatory processes that governed the compartmentalization of the β_1-ARs and other GPCRs. These proteins are divided into two types. The first are accessory compartmentalizing proteins such as SAP97 and AKAP5, which are involved in regulating the localization of β-adrenergic receptors (β-ARs) in the cell and in compartmentalization of cAMP, respectively (Gardner et al., 2006, 2007; Valentine and Haggie, 2011; Nooh et al., 2013). Endosomal proteins such as the PDZ protein sorting nexin-27 (SNX27) represent the second class, which are involved in the redistribution of the agonist-internalized GPCR from endosomes to the plasma membrane (Seaman et al., 2013).

These paradigms were identified in mammalian cells, but their general validity to β_1-AR compartmentalization in complex cells such as adult rat ventricular myocytes (ARVMs) is unknown. ARVMs contain an extensive network of transverse tubules (T-tubules) and their juxtaposed sarcoplasmic reticula, as well as an extensive set of sarcomeres, which alone represent 45%–60% of the cardiomyocyte volume (Bers, 2001). While ARVMs express both β_1-AR and β_2-AR, the β_1-AR complement was involved in PKA-mediated effects on contractility and in inducing hypertrophy and cardiomyocyte apoptosis (Morisco et al., 2001; Xiao, 2001; Zhu et al., 2001). A better characterization of the role of barcodes on spatiotemporal localization and redistribution of β_1-AR in ARVMs would provide crucial new information on the factors that regulate compartmentalization and subsequent signaling of cardiac β_1-AR.

Material and Methods

Adult Rat Ventricular Myocytes Cultures. Animal experiments were performed according to protocols that were approved by the University of Tennessee–HSC Institutional Animal Care and Use Committee. Studies conformed to the *Guide for Care and Use of Laboratory Animals* published by the U.S. National Institutes of Health (Publication No. 85-23, revised 1996, https://grants.nih.gov/grants/.../guide-for-the-care-and-use-of-laboratory-animal). Sprague-Dawley rats (200–250 g) were heparinized and anesthetized with 4% isoflurane. The hearts were excised, cannulated on a Langendorff apparatus, and then perfused for 5 minutes with oxygenated modified perfusion buffer composed of 133 mM NaCl, 4 mM KCl, 11 mM glucose, 1.2 mM NaH_2PO_4, 1.2 mM $MgCl_2$, and 10 mM HEPES (pH 7.4 with NaOH), and supplemented with 0.1% butanedione monoxime until the blood cleared (Louch et al., 2011). Thereafter, the heart was perfused with perfusion buffer supplemented with 0.1% collagenase type II (CLS2; Worthington, Lakewood, NJ) for 20 minutes to break down the extracellular matrix. The enzymatically digested ventricles were minced and gently shaken in perfusion buffer supplemented with 0.2% bovine serum albumin. Undigested ventricular tissue was removed using a 250-μm-mesh sieve. Then, the concentration of Ca^{2+} was increased stepwise to 0.5 mM in perfusion buffer containing 0.2% bovine serum albumin. The cells were concentrated by centrifugation and resuspended in culture media composed of (per liter) 9.3 g of Medium-199 Powder (Sigma-Aldrich, St. Louis, MO), 5 mM creatine, 2 mM carnitine, 5 mM taurine, 10 mM $NaHCO_3$, 10 mM HEPES (pH 7.4), and 100 U/ml penicillin plus 100 μg/ml streptomycin. Rod-shaped ventricular myocytes were counted with a hemocytometer, and ~40,000 cells were plated onto laminin-coated (10 μg/ml) coverslips in tissue culture dishes. After 12 hours, the medium was aspirated and the myocytes were infected with 50 multiplicities of infection with adenoviruses harboring the desired construct for 6 hours. All confocal imaging experiments were conducted on cells that were fixed within 72 hours from preparation to minimize ongoing morphologic changes in cardiomyocytes during culture (Banyasz et al., 2008; Pavlović et al., 2010).

Antibodies, siRNA, and Additional Reagents. Cy3-labeled anti-FLAG M2 monoclonal antibody was obtained from Sigma. Polyclonal rabbit anti-FLAG IgG and CF-350, CF-543, and CF-633; CF-770-conjugated anti-rabbit IgG and anti-mouse IgG; and Di-8-ANEPPS were obtained from Biotium (Fremont, CA). Monoclonal anti-SAP97 was obtained from Enzo Life Sciences (Farmingdale, NY), while H-89 and myristoylated PKA-inhibitor peptide (mPKI) 14-22 amide were obtained from EMD-Millipore (Billerica, MA). *st*-Ht31 and *st*-Ht31-*pro* were obtained from Promega (Fitchburg, WI). Anti-$SNX27_{(366-415)}$ (ab178388) and anti-β-actin (ab8226 and ab8227) were obtained from Abcam (Cambridge, MA). The adenovirus (Ad) containing short hairpin RNA (shRNA) for rat SAP97 (shSAP97) sense 5′-GATATC-CAGGAGCATAAAT-3′ was kindly provided by M. B. Anumowno, SUNY Upstate Medical University, Syracuse, NY (Vaidyanathan et al., 2010). The sequence between 861 and 881 in AKAP150 (AAGAAGACAAAATC-CAAACTT) or its inactive control (GTCTCCACGCGCAGTACATTT) was used to generate the AKAP150-specific shRNA (shAKAP5) in adenovirus. Adenoviruses pAd5CMV-NpA harboring the wild-type (WT) β_1-AR, β_1-AR deleted PBM (ΔPDZ), mutation of Ser^{312} to alanine (S312A) β_1-AR, were previously described (Li et al., 2013). These viruses were generated, purified, and tittered at the Vector Core of the University of Tennessee Health Sciences Center.

Acid Strip Confocal Microscopy and Dual Microscopy Protocols. Cardiomyocytes in serum-free culture medium were incubated with either Cy3-conjugated to monoclonal anti-FLAG M2 IgG or with unconjugated rabbit anti-FLAG IgG (4 μg/ml) for 1 hour at 37°C. In some experiments diluents, 0.3 μM H-89, mPKI, or 50 μM *st*-Ht-31 peptides was added in the middle of the antibody incubation step. ARVMs were exposed to 10 μM isoproterenol (ISO) for 30 minutes at 37°C to activate the receptor and promote the redistribution of the agonist-mediated β_1-AR. Then, the slides were chilled on ice and exposed to 0.5 M NaCl and 0.2 M acetic acid (pH 3.5) for 4 minutes on ice to strip antibody bound to the FLAG-tag of extracellularly oriented FLAG-tagged β_1-AR (Ehlers, 2000; Snyder et al., 2001; Delos Santos et al., 2006). Cultures were quickly rinsed in warm culture medium and incubated in culture medium supplemented with 100 μM of the β-antagonist alprenolol (ALP) at 37°C for 60 minutes to promote the redistribution of the agonist-exposed β_1-AR. After each time period, cover slips were either acid stripped as described previously, or rinsed and fixed in phosphate-buffered saline containing 4% paraformaldehyde and 4% sucrose (pH 7.4) for 10 minutes at room temperature. To permeabilize the myocytes, fixed slides were incubated in HEPES-buffered saline solution containing 0.2% Triton X-100 for 10 minutes at 4°C (Li et al., 2013).

At this stage, coded slides that were incubated with Cy3-anti-FLAG IgG were examined by confocal microscopy using Cy3 (λ_{ex} 550 nm, λ_{em} 570 nm) and 4′,6-diamidino-2-phenylindole (λ_{ex} 358 nm, λ_{em} 461) channels and their pseudo fluorescence red for Cy3 and pseudo fluorescence violet results for 4′,6-diamidino-2-phenylindole are presented. To label the β_1-AR in cells that were incubated with rabbit anti-FLAG IgG, the slides were exposed to a 1:500 dilution of fluorescent anti-rabbit IgG for 30 minutes in blocking buffer prior to their examination by confocal microscopy. Permeabilized slides for dual confocal microscopy were incubated with 1:1000 dilution of the primary antibody under study (such as anti-SAP97 or anti-SNX27) for

30 minutes at 37°C, washed and incubated with 1:500 dilution of fluorescent anti-mouse or anti-rabbit IgG, and then analyzed by confocal microscopy. Confocal fluorescence microscopy was performed at room temperature on coded slides and optical section thicknesses of 1.0 μm images were acquired by an Olympus FV1000 confocal microscope equipped with 40 or 60 Å oil immersion (numerical aperture 1.30) objective lens, using FV10-ASW 3.1 acquisition software (Olympus, Center Valley, PA). (Nooh and Bahouth, 2017). TIFF files of each image were exported and analyzed for pixel intensity and distribution by ImageJ software (https://imagej.nih.gov/ij/). Each cell was partitioned by a line, every point of which was at a distance of 400 nm from the outer periphery of the ARVMs, using the ImageJ software. This line formed the outer limit of the area used to index pixel intensity of internal β_1-ARs in a given cell, while the area formed between the peripheral cell membrane and this line was used to index the distribution of pixels associated with cell surface β_1-ARs (Gardner et al., 2004, 2006, 2007; Li et al., 2013; Nooh and Bahouth, 2017).

Radioligand Binding and Western Blotting Procedures. Radioligand binding was carried out on whole cell homogenates prepared from ARVMs that were infected with either the empty adenoviral vector or the WT β_1-AR expressing virus. ARVMs were scrapped, concentrated by centrifugation, and homogenized in hypotonic lysis buffer (50 mM HEPES, pH 7.4 and 10 mM $MgCl_2$) supplemented with 1X cOmplete protease inhibitor cocktail (Sigma-Aldrich, St. Louis, MO). Saturation binding experiments involved mixing equal amounts of protein (5 μg) prepared from different ARVMs with 5–200 pM (^{125}I)Iodocyanopindolol in duplicate in the absence or presence of 100 μM ISO as described previously (Delos Santos et al., 2006). The K_D and the B_{max} values for (^{125}I)Iodocyanopindolol binding were estimated by parametric fitting of the data using the Prism 7 software (GraphPad Software Inc., San Diego, CA).

For western blotting, ARVMs expressing the appropriate construct were lysed in lysis buffer composed of: 150 mM NaCl, 50 mM Tris, pH 8.0, 5 mM EDTA, 0.2% Triton X-100, 10 μg/ml leupeptin, 10 μg/ml aprotinin, 10 μg/ml chymostatin, and 1 mM phenyl methyl sulfonyl fluoride for 1 hour at 4°C. Then, insoluble cellular debris was removed by centrifugation at 14,000*g* for 15 minutes at 4°C. After equalizing protein concentrations across all samples, lysates in 2X-Laemmli sample buffer were subjected to SDS-PAGE under denaturing conditions and electroblotted to nitrocellulose. Identical gels were run and transferred for separate detection of the desired protein by western blotting, as described previously (Nooh and Bahouth, 2017).

Statistics. Data were derived from image analysis that determined specific total pixels and pixels outside versus inside the 400-nm partition that was drawn around the inner circumference of cardiomyocytes. The ratio of pixels residing outside the 400-nm partition to that of the percentage of total pixels was calculated for each image. The average ± S.E. of percentile pixel ratios from three separate experiments derived from 10 images/experiment (n = 30 images) is presented. Statistical comparison between two groups was performed by unpaired t tests and for multiple groups by analysis of variance (ANOVA) followed by Bonferroni's test with a single pooled variance test in which the family-wise error rate was set at 0.05, using GraphPad Prism 7 software (GraphPad Software Inc.).

Results

Spatiotemporal Localization of the Human β_1-AR in ARVMs. The ARVMs used in this study were maintained in defined media without serum to minimize their transformation and all experiments were carried out within 72 hours after their isolation (Banyasz et al., 2008). Under these conditions, cardiomyocytes maintained their rod-shaped appearance and parallel myofibrillar architecture for several days (Simpson et al., 1999). Our studies were carried out by adenoviral-mediated expression of an N-terminally modified WT β_1-AR that expressed the FLAG epitope (FLAG-tagged WT β_1-AR) because there were no antibodies we could find that would detect native β_1-AR in mammalian cells. Radioligand binding studies indicated that infection of ARVMs with 50 multiplicities of infection of either control or WT β_1-AR-expressing adenovirus increased the B_{max} value of β-AR from 112 ± 19 to 216 ± 43 fmol/mg protein with a K_D value of 19 ± 6 pM (n = 5). Cardiomyocytes infected with the WT FLAG-β_1-AR adenovirus were incubated with Cy3-labeled anti-FLAG IgG to label the β_1-AR, and then fixed and monitored by confocal microscopy (Fig. 1). The images were exported as TIFF files into the ImageJ software and analyzed for pixel distribution outside and inside a 400-nm partition drawn around the inner circumference of the ARVMs.

In quiescent ARVMs, 79% ± 12% Cy3-conjugated anti-FLAG IgG pixel intensities (pseudo red fluorescence in Fig. 1A, images a and a′) were localized outside the 400-nm partition ($P < 0.05$ compared with inside the partition), indicating that WT β_1-ARs were expressed at the plasma membrane of ARVMs. The orientation of Cy3 fluorescence, which indexes the orientation of the FLAG epitope, was determined by an acid wash procedure applied to intact cells prior to fixing (Fig. 1A, image b). This procedure would strip the fluorescent anti-FLAG antibody bound to the extracellular FLAG epitope. The acid wash procedure expunged 73% ± 9% of total Cy3 fluorescence, indicating that the majority of β_1-ARs were confined at the surface sarcolemma membrane of ARVMs.

Exposing ARVMs to a high concentration of the β-agonist ISO resulted in redistribution of membranous Cy3 fluorescence into numerous small punctate structures throughout the cell (Fig. 1A, images c and c′). The fluorescence of the Cy3 puncta outside versus inside the 400-nm divider accounted for 13% ± 5% versus 86% ± 11% of the total pixel intensities, respectively, and these differences were statistically significant ($P < 0.05$). Treatment of these cells with a mild acid wash removed 8.7% ± 3% of the pixels, indicating that Cy3 pixels were intracellularly in an acid inaccessible compartment (Fig. 1A, image d).

Replacing ISO with the β-blocker ALP induced the translocation of the WT β_1-AR from inside to outside the 400-nm partition (Fig. 1A, images e and e′). Under these conditions, fluorescence outside the 400-nm partition accounted for 74% ± 9% of total pixel intensity ($P < 0.05$, compared with inside the divider). The amount of Cy-3 fluorescence that was stripped by acid wash in these ARVMs amounted to 66% ± 8%, indicating that ALP induced the redistribution of punctal WT β_1-AR to the surface membrane (Fig. 1A, image f). Statistical comparisons were made between the Cy3 pixel distributions by the partition method versus the acid-strip procedure in untreated ARVMs by ANOVA followed by Bonferroni's test (Fig. 1B). These analyses showed statistically insignificant differences ($P > 0.05$) between the percentile distribution of pixels outside the 400-nm partition (the image a condition in Fig. 1A) compared with the percentile of fluorescence stripped by the acid wash method in untreated control ARVMs (the image b condition in Fig. 1A). Moreover, no statistically significant difference ($P > 0.05$) occurred when the percentile of Cy3 pixels outside the 400-nm partition in ISO/ALP ARVMs were compared with the percentile of fluorescence stripped by the acid wash method in ISO/ALP-treated ARVMs (Fig. 1B). These findings indicate that the partition method is a valid

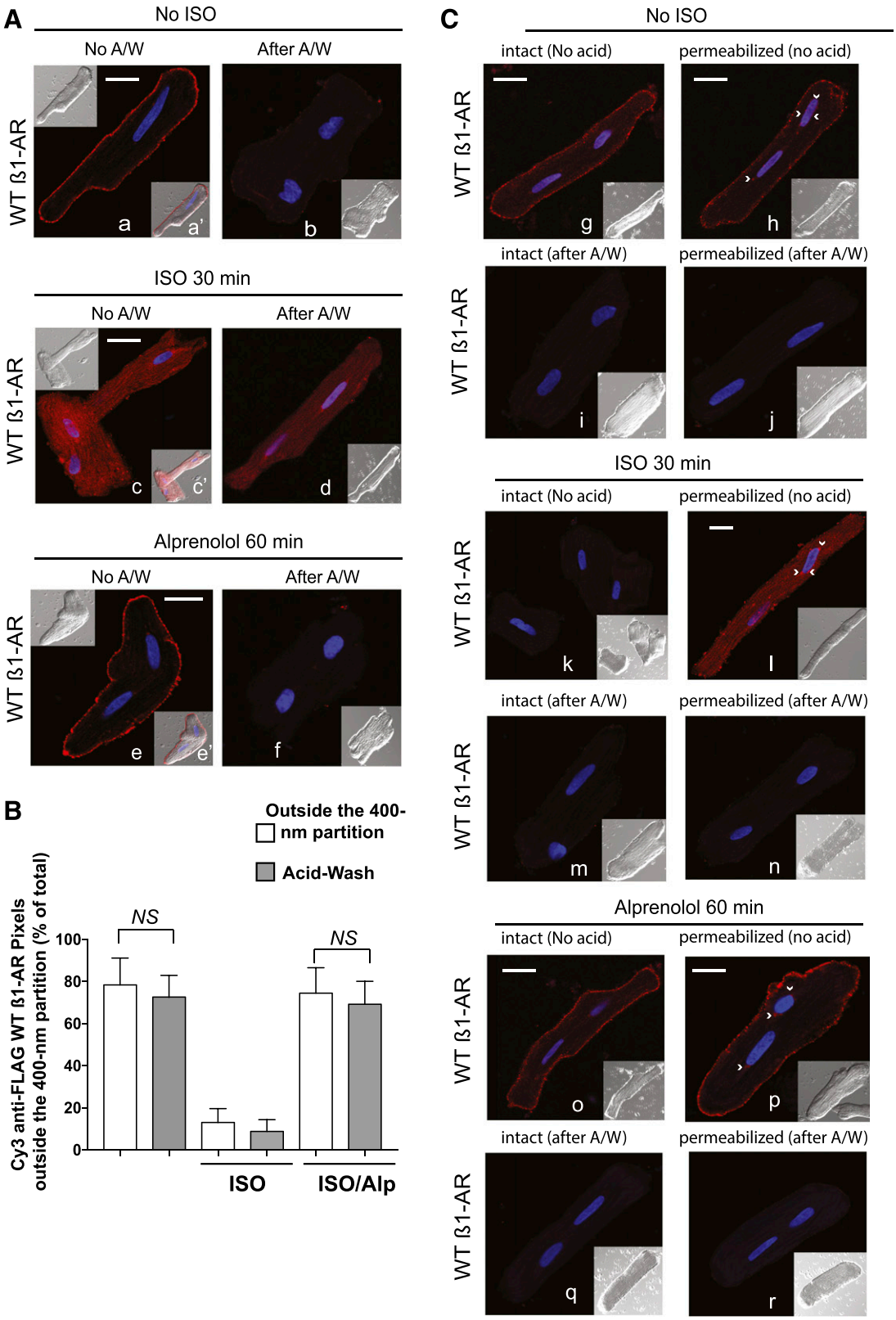

Fig. 1. Compartmentalization of WT β_1-AR in ARVMs. (A) ARVMs expressing the FLAG-tagged human WT β_1-AR were prelabeled for 1 hour with Cy3-anti-FLAG antibody and fixed (image a). The rest of the slides were exposed to 10 μM ISO for 30 minutes, fixed (image c) or washed and incubated with 100 μM ALP for 1 hour, and fixed (image e). Slides corresponding to images a, c, and e were subjected to a mild acid wash prior to fixing (images b, d, and f). Cells were imaged and pseudo fluorescence of Cy3 (red) and 4′,6-diamidino-2-phenylindole (violet) is presented. Nomarski image or Cy3-superimposed to the Nomarski image are presented in the upper left or in the right lower quadrant, respectively. (B) Cy3 pixel distribution (mean ± S.E. from a total of 30 images derived from three separate experiments) in ARVMs that were untreated and exposed to ISO or ISO/ALP by the microscopic partition vs. the acid-strip procedure were analyzed by one-way ANOVA followed by Bonferroni's test with a single pooled variance test. NS, indicates nonsignificant differences between the column pairs. (C) Intact or permeabilized ARVMs prepared as in (A), were incubated with buffer (images g–j),

approach for compartmental analysis of GPCR distribution in ARVMs.

We conducted additional studies to determine the distribution of the WT β_1-AR in intact versus permeabilized naive or ISO-treated ARVMs (Fig. 1C, images g and h, respectively). Staining permeabilized naive ARVMs with Cy-3 anti-FLAG revealed additional limited amounts of β_1-AR staining around the nuclei (Fig. 1C, arrows in image h). The mild acidic wash stripped the Cy3 fluorescence from these cells, indicating that Cy3 staining was limited to the plasmalemmal membrane in intact or permeabilized naive ARVMs (Fig. 1C, images i and j). Staining ISO-exposed intact or permeabilized cardiomyocytes with Cy3-anti-FLAG IgG revealed that β_1-AR staining in permeabilized ISO-exposed ARVMs, but not in intact ISO-exposed ARVMs (Fig. 1C, compare image k to image i). These findings suggest that ISO induced the redistribution of the WT β_1-AR into compartments in ARVMs that were inaccessible to staining with Cy3-labeled anti-FLAG IgG. As expected, the acid wash procedure stripped Cy3 fluorescence from permeabilized ISO-treated ARVMs (Fig. 1C, images m and n). Finally, we determined the effect of ALP on the distribution of the WT β_1-AR in intact ISO-exposed versus permeabilized ISO-exposed ARVMs (Fig. 1C, images o–r). Cy-3 staining of intact or permeabilized ISO/ALP-treated myocytes was limited to the surface cell membrane (Fig. 1C, images o and p, respectively), and was stripped by mild acid treatment (Fig. 1C, images q and r). Therefore, it appears that WT β_1-AR redistributed from an acid-inaccessible compartment to an extracellularly exposed compartment in response to ALP.

Characterization of the Compartment Harboring the WT β_1-AR in Agonist-Exposed ARVMs. Membranous GPCR translocate from their membranous compartment to intracellular early endosomes in response to agonist via two main redistribution pathways, namely, clathrin coat–mediated endocytosis and caveolar mechanisms (Baig et al., 2002; Pelkmans et al., 2004; Wolfe and Trejo, 2007) (Fig. 2A). The average diameter of the puncta harboring the ISO-activated WT β_1-AR in ARVMs was ~230 ± 50 nm (n = 30, Fig. 1). This diameter is smaller than the diameter of early endosomal vesicles, which varies from 250 to 400 nm for small diameter smooth vesicles to ~600–900 nm for large endocytic vesicles with tubular extensions (Wileman et al., 1985; Jean-Alphonse et al., 2014).

We conducted colocalization studies between the WT β_1-AR and the PDZ protein SNX27, which is an early endosome resident protein expressed in ARVMs (Fig. 2B). SNX27 is universally involved in recycling of PBM-containing cargoes, such as β_1-AR, β_2-AR, and many other GPCRs from early endosomes to the plasma membrane (Lauffer et al., 2010; Steinberg et al., 2013). Distribution of SNX27 and the WT-β_1-AR in control versus ISO-treated and permeabilized ARVMs revealed that while SNX27 was colocalized with the WT β_1-AR in naive ARVMs, its distribution was significantly different from that of the WT β_1-AR in ISO-exposed ARVMs (Fig. 2, C and D). In ISO-exposed ARVMs, SNX27 was confined to the cytosolic side of the cardiac plasmalemmal membrane (pseudo green in Fig. 2C), while the WT β_1-AR was distributed in puncta throughout the ARVMs (pseudo red in Fig. 2C).

The diameter of β_1-AR puncta, however, was close to the diameter of T-tubules, which are plasma membrane tubular invaginations that rapidly propagate excitatory signals to inside cardiomyocytes through tubules with diameters between 180 and 280 nm (Soeller and Cannell, 1999). To find out if these structures were colocalized, we performed dual-fluorescence microscopy on ARVMs that expressed the WT β_1-AR and the T-tubule-specific fluorescent dye Di-8 ANEPPS (Lyon et al., 2009). A problem encountered in using Di-8 ANEPPS was its broad excitation/emission spectra (λ_{ex} = 498 nm and λ_{em} = 713 nm), which overlapped with the wavelength maxima of Cy3 (λ_{ex} = 550 nm and λ_{em} = 570 nm) and many other fluorescent dyes. Therefore, we used fluorescent dyes with nonoverlapping excitation and emission spectra, such as CF-350 (absorbance/emission maxima: 347/448 nm) or CF-770 (absorbance/emission maxima: 770/797 nm) that were conjugated to goat anti-rabbit IgG. We verified by western blotting that the polyclonal rabbit anti-FLAG IgG selectively and quantitatively recognized the M_r = 66–70 kDa mature form of the FLAG-tagged WT β_1-AR in cell lysates prepared from HEK-293 cells stably expressing the FLAG WT β_1-AR (Fig. 2E).

To detect the β_1-AR and Di-8 ANEPPS by dual-fluorescence confocal microscopy in ARVMs, cell expressing FLAG-β_1-AR were exposed to ISO, fixed, and incubated with Di-8 ANEPPS for 10 minutes. The slides were washed, permeabilized, and incubated with rabbit anti-FLAG IgG to label the β_1-AR, followed by CF-350 or CF-770-conjugated to goat anti-rabbit IgG. In ISO-treated ARVMs, CF-350-labeled WT β_1-AR (pseudo violet in Fig. 2F, image a) and Di-8 ANNEPS (pseudo green in Fig. 2F, image b) were largely colocalized by >87% ± 12% ($P > 0.05$ from 30 images derived from n = 3 experiments). Similar findings were obtained with the CF-770 conjugated anti-FLAG IgG as well (Fig. 2F, images a′–d′).

Barcoding of β_1-AR Trafficking in ARVMs. In mammalian cells, specific barcodes, such as the PBM and PKA-substrate Ser^{312} are involved in translocating endosomal WT β_1-AR back to plasma membrane, but whether these barcodes are also involved in the redistribution of β_1-AR in ARVMs is unknown (Nooh and Bahouth, 2017). ARVMs were infected with adenovirus harboring either the PBM inactivated β_1-AR (β_1-ARΔPDZ) or a β_1-AR construct with a Ser^{312} to Ala^{312} [(S312A) β_1-AR] inactivating point mutation (Gardner et al., 2004, 2006; Li et al., 2013). In untreated myocytes, Cy3 labeled β_1-ARΔPDZ or (S312A) β_1-AR were localized by 79% ± 12% and by 83% ± 14%, respectively, at the surface membrane of naive ARVMs (Fig. 3A, images a and a′ and images c and c′, respectively; Fig. 3B) and their fluorescence was expunged after exposing these cells to a mild acid treatment (Fig. 3A, images b and d, respectively). Exposing these ARVMs to ISO, redistributed 83% ±13% of β_1-ARΔPDZ and 86% ± 15% of (S312A) β_1-AR into puncta inside the 400-nm partition (Fig. 3A, images e and e′ and images g and g′, respectively; Fig. 3B).

ISO 30′ (images k–n), or ISO/ALP (images o–r) as described in *Material and Methods*. These slides were incubated with Cy3-anti-FLAG IgG for 1 hour and exposed to neutral (images g, h, k, l, o, and p) or acidic buffer (images i, j, m, n, q and r), and then fixed and visualized by confocal microscopy. Each scale bar in (A) and (B) represents 15 μm. Small arrows indicate nuclear fluorescence.

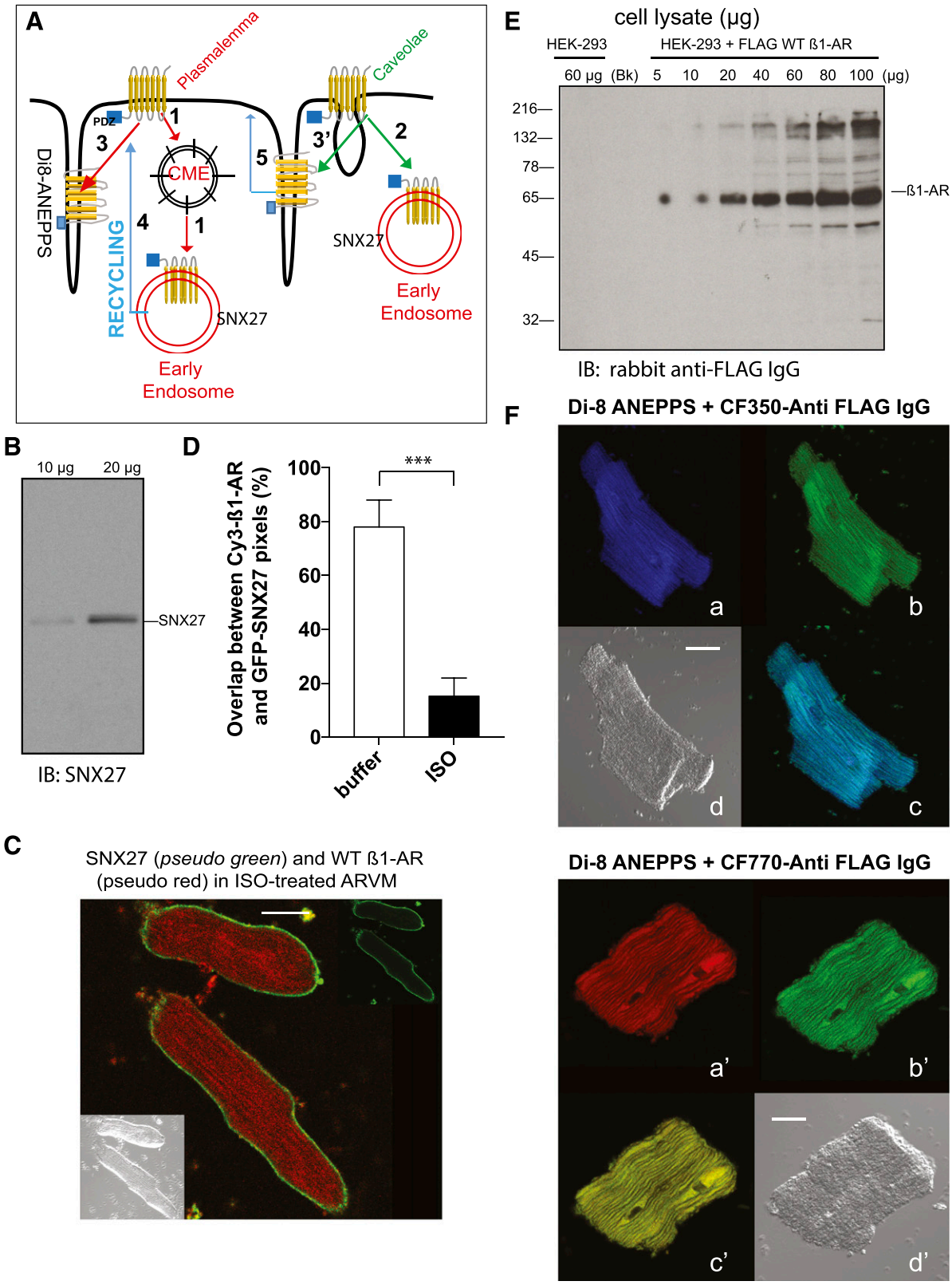

Fig. 2. Fluorescence colocalization microscopy between WT β_1-AR and intracellular markers in ARVMs. (A) Cartoon representing modes of agonist-mediated GPCR internalization. The majority of GPCRs are endocytosed from the surface membrane to early endosomes by clathrin-mediated endocytosis into early endosomes (number 1), or from caveolae into early endosomes (number 2). The cartoon also indicates that GPCRs may translocate to T-tubules, which are continuous with the plasma membrane in agonist-exposed ARVMs (number 3). Specific markers for early endosomes and T-tubules, such as SNX27 and Di-8 ANEPPS, respectively, may provide clues about the intracellular compartment harboring the β_1-AR in ISO-exposed ARVMs. Also depicted are possible mechanisms for GPCR recycling from their intracellular compartment back to the surface membrane (number 4) or caveolae (number 5). (B) Western blotting of 10 or 20 μg of ARVM cell lysates with anti-SNX27. (C) Colocalization between CF-770 labeled WT β_1-AR (pseudo red) and GFP-labeled SNX27 (pseudo green) in ISO-exposed ARVMs. The scale bar represents 20 μm. (D) Statistical comparison of CF-770 vs.

The fluorescence of these cells was resistant to mild acid exposure (Fig. 3A, images f and h, respectively). The distribution of β_1-ARΔPDZ or (S312A) β_1-AR overlapped with the distribution of Di-8 ANEPPS in ISO-treated ARVMs (Fig. 3C, images m–o and q–s, respectively, from 30 images derived from $n = 3$ separate experiments). Punctal distribution of β_1-ARΔPDZ or (S312A) β_1-AR did not change significantly ($P > 0.05$) upon replacing ISO with ALP (Fig. 3A, images i and i′ and images k and k′, respectively; Fig. 3B), and their fluorescence was not affected by exposure to a mild acid solution (Fig. 3A, images j and l, respectively). Therefore, these two mutations in the β_1-AR markedly inhibited its redistribution from the acid-resistant compartment back to the surface sarcolemmal membrane.

Involvement of PKA and PKA-AKAP Interactions in β_1-AR Trafficking in ARVMs. The involvement of PKA or AKAP-PKA interactions on the distribution of β_1-AR in ARVMs was determined using PKA or PKA-AKAP interaction inhibitors (Fig. 4). Inhibition of PKA with the mPKI or disruption of PKA-AKAP interactions with the cell-permeable *st*-Ht31 peptide did not affect the localization of Cy-3 labeled WT β_1-AR in naive ARVMs (84% ± 12% and 79% ± 11% of the pixels were distributed outside the partition, respectively, as illustrated in Fig. 4, B and C. These pixels redistributed toward the inside of this partition (84% ± 16% and 83% ± 15%, respectively) in response to ISO (Fig. 4A, images a and b, d and e, g and h, and j and k; Fig. 4, B and C). However, inactivation of PKA prevented the translocation of the ISO-exposed WT β_1-AR from inside to outside the partition in response to ALP (Fig. 4A, compare the pixel distribution in image c to that in images f and i and the graphical data in Fig. 4B). In ARVMs that were pretreated with *st*-Ht31-*pro*, which is the inactive counterpart of *st*-Ht31, ALP induced the redistribution of WT β_1-AR pixels from inside (88% ± 16%) into the region outside the 400-nm barrier by 84% ± 13% (Fig. 4A, image i; Fig. 4C). However, internal pixels in ARVMs that were pretreated with *st*-Ht31 did not redistribute to the cell surface membrane in response to ALP (compare images k–l in Fig. 4A). In buffer or *st*-Ht31-*pro* pretreated myocytes, replacing ISO with ALP induced significant redistribution of β_1-AR pixels from inside to outside the 400-nm partition (Fig. 4, B and C, $P < 0.001$ by one-way ANOVA followed by Bonferroni's analysis). However, ALP failed to induce the translocation of WT β_1-AR from inside to outside the 400-nm partition in mPKI or *st*-Ht-31 pretreated myocytes (Fig. 4, B and C, $P > 0.05$ by one-way ANOVA followed by Bonferroni's analysis).

Involvement of the PDZ Protein SAP97 on β_1-AR Redistribution in ISO-Exposed ARVMs. In addition to PKA-AKAP interactions, the PDZ protein SAP97 was involved in translocation of the agonist-internalized β_1-AR from endosomes to the plasma membrane of mammalian cells (Li et al., 2013; Nooh et al., 2014; Nooh and Bahouth, 2017). SAP97 is a PDZ scaffolding protein that is localized at the cytoplasmic side of the surface membrane of ARVMs (Shcherbakova et al., 2007). SAP97 is expressed in ARVMs cells as a ~110 kDa protein (Fig. 5A), and its expression was effectively reduced by >85% after infecting these cells with an adenovirus harboring a highly effective and validated shRNA to SAP97 (Fig. 5A, compare lane 2 with lane 3). In naive ARVMs expressing either the scrambled Ad-shRNA or the SAP97 Ad-shRNA, 88% ± 15% and 80% ± 13% of WT β_1-AR pixels were distributed outside the 400-nm partition, respectively (Fig. 5B, images a and d, respectively). These findings indicate that downregulation of SAP97 did not affect the compartmentalization of WT β_1-AR in ARVMs. ISO induced the redistribution of the WT β_1-AR from the surface plasmalemmal membrane into puncta inside the 400-nm partition by 85% ± 15% in scrambled Ad-shRNA-infected ARVMs and by 88% ± 13% in SAP97 Ad-shRNA-infected ARVMs ($P > 0.05$ derived from 30 images/condition similar to those in Fig. 5B, images b and e, respectively). In ARVMs infected with scrambled Ad-shRNA, 85% ± 10% of WT β_1-AR puncta redistributed back to the cell membrane (outside the 400-nm partition) upon replacing ISO with ALP (Fig. 5B, image c). However, in ARVMs that were infected with SAP97 Ad-shRNA, more than 85% of the WT β_1-AR fluorescence remained inside the 400-nm partition. Comparisons of pixel distribution between 30 images per condition, indicated that knockdown of SAP97 significantly inhibited the redistribution of β_1-AR puncta to the cell membrane of ARVMs compared with its scrambled control Ad-shRNA (Fig. 5C).

Dual-fluorescence microscopy indicated that in permeabilized ARVMs, SAP97 was confined to the cytosolic side of the surface membrane in buffer or in ISO-treated ARVMs (pseudo green in Fig. 5D) and colocalized with the WT β_1-AR in naive ARVMs (Fig. 5E). However, in ISO-exposed ARVMs, the WT β_1-AR was localized in puncta distributed throughout the ARVMs (pseudo red in Fig. 5D) and its distribution was significantly different ($P < 0.05$) from that of SAP97 (Fig. 5E).

Discussion

Characterization of the Compartmentalization of β_1-AR in ARVMs. Spatial localization of β-ARs and vectoring their signaling to specific intracellular compartments through compartmentalization are thought to play a major role in the development of heart diseases, such as heart failure (Head et al., 2005; Fischmeister et al., 2006; Lyon et al., 2009; Nikolaev et al., 2010). Assessment of the precise distribution of β-ARs in the heart by direct visualization is

GFP pixel overlap (mean ± S.E. from 30 images derived from three separate experiments) in ARVMs that were untreated (buffer) or exposed to ISO for 30 minutes. Statistical comparisons in the percentile of overlapping pixels between the two groups were carried out by student's *t* test. *P* values are expressed as nonsignificant to indicate no significant difference or *, **, and *** to indicate $P < 0.05$, $P < 0.01$, and $P < 0.001$, respectively. (E) Western blotting of increasing amounts of cell lysates prepared from HEK-293 stably expressing FLAG-β_1-AR that were probed with rabbit polyclonal anti-FLAG IgG. (F) ARVMs expressing the WT FLAG β_1-AR were incubated with 5 μg/ml of rabbit anti-FLAG IgG for 1 hour and then exposed to buffer or ISO for 30 minutes as described in Fig. 1A. These slides were incubated with 10 μM Di-8 ANEPPS, washed, and then fixed. Slides were permeabilized and incubated with CF350- (*a–d*) or CF770-goat anti-rabbit IgG (images a′–d′) for 30 minutes and visualized by confocal microscopy. Di-8 ANEPPS staining (pseudo green in images b and b′) and Nomarski images (images d and d′) are shown. Distribution of fluorescent pixels for CF-350 (pseudo violet in image a) or CF-770 (pseudo red in image a′) were superimposed on Di-8 ANEPPS staining (pseudo cerulean or yellow in images c and c′, respectively). Each scale bar in (A) and (B) represents 10 μm.

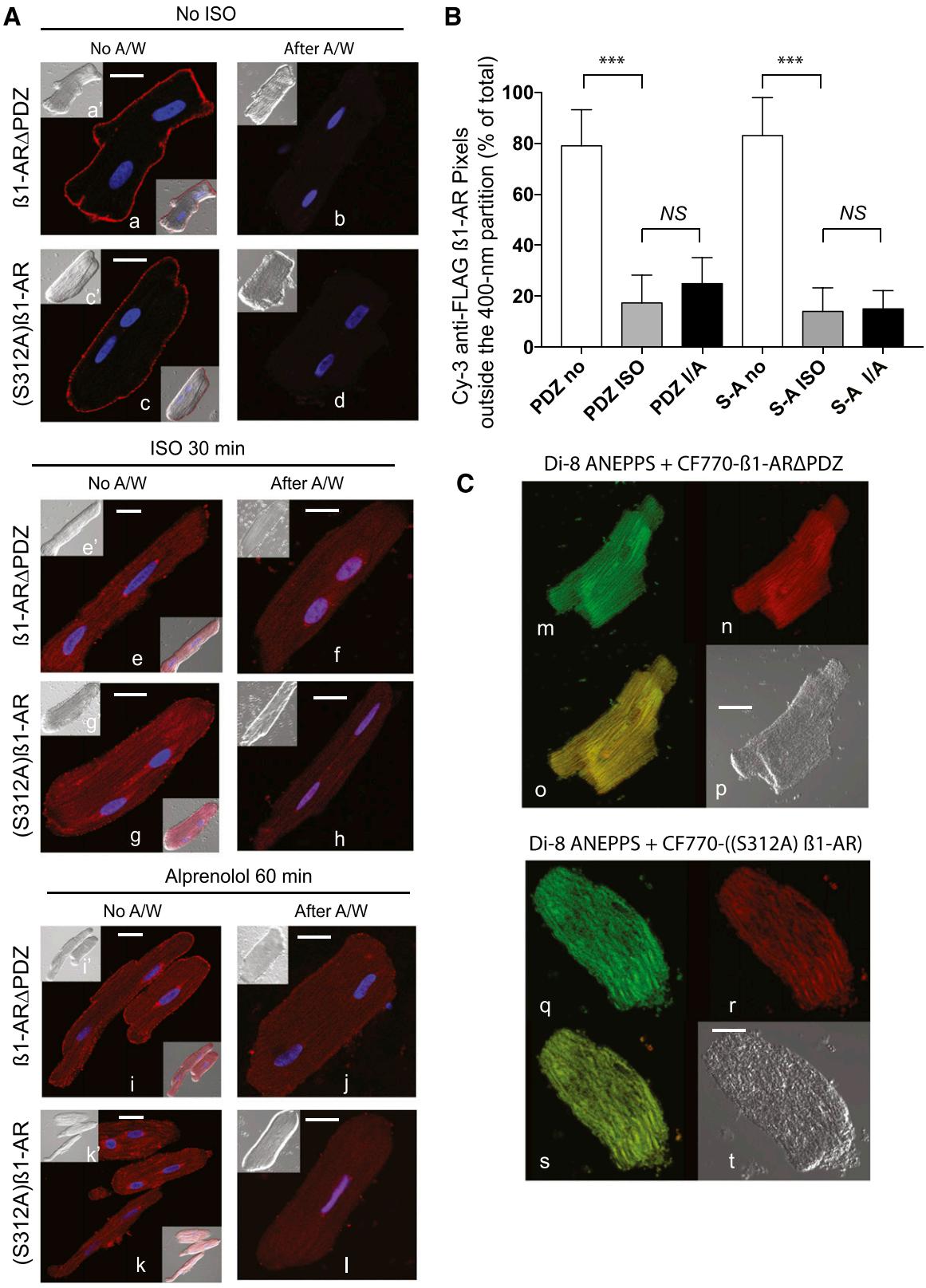

Fig. 3. Compartmentalization of β_1-ARΔPDZ and (S312A) β_1-AR in ARVMs. (A) Confocal microscopy of FLAG β_1-ARΔPDZ or FLAG (S312A) β_1-AR in ARVMs was carried as previously described in Fig. 1A. Each scale bar in (A) represents 15 μm. (B) Pixel distribution of Cy3 β_1-AR ΔPDZ (PDZ) or Cy3-[(S312A) β_1-AR] (S-A) outside the 400-nm partition (mean ± S.E.) of ARVMs that were untreated and exposed to ISO or ISO/ALP by the microscopic partition procedure from 30 images/condition that were derived for three separate experiments is presented. Statistical comparisons were carried out by one-way ANOVA followed by Bonferroni's test. NS, indicates nonsignificant differences between the column pairs or *, **, and *** to indicate $P < 0.05$, $P < 0.01$, and $P < 0.001$, respectively. (C) ARVMs expressing FLAG-β_1-AR ΔPDZ or FLAG (S312A) β_1-AR were processed as described in Fig. 2F. Slides were permeabilized and incubated with CF770-goat anti-rabbit IgG and visualized. β_1-ARΔPDZ staining (pseudo red, image n) or (S312A) β_1-AR (pseudo red, image r) and that of with Di-8 ANEPPS (images m and q) were superimposed (images o and s, respectively). Each scale bar in (A) and (B) represents 15 μm.

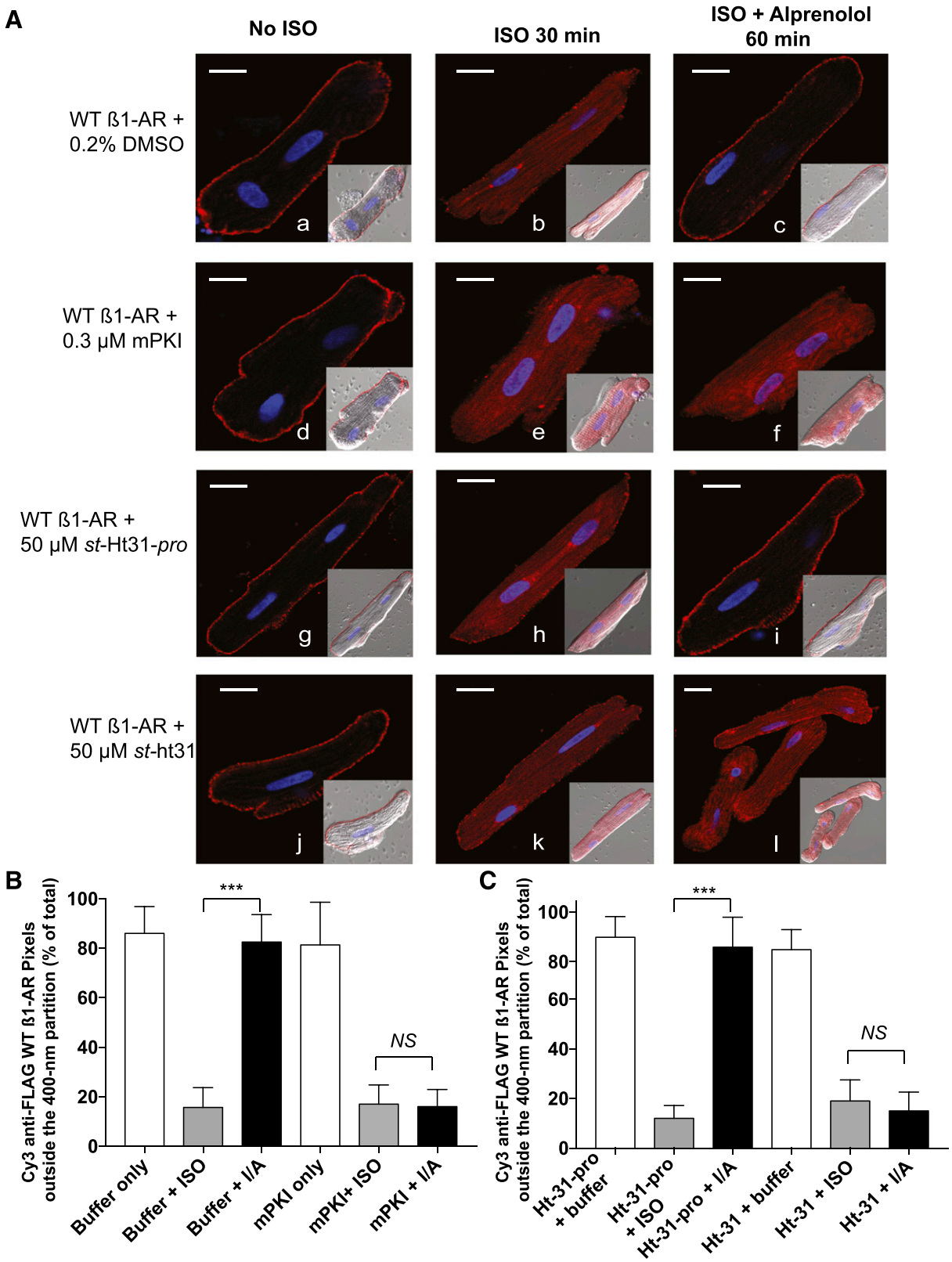

Fig. 4. Effect of mPKI and *st*-Ht-31/pro on compartmentalization of WT β_1-AR in ARVMs. (A) ARVMs expressing the FLAG-tagged WT β_1-AR were exposed to Cy3-anti-Flag antibody and pretreated for 30 minutes either with buffer (images a–c), 0.3 μM mPKI (images d–f), 50 μM *st*-Ht-31-pro (images g–i), or 50 μM *st*-Ht-31 (images j–l). The indicated slides were exposed to ISO or ISO/ALP as described in Fig 1A. The distribution of fluorescent pixels in confocal images (pseudo red) is shown alone or superimposed on the Nomarski image in the right lower quadrant. Each scale bar represents 15 μm. (B) Pixel distribution of Cy3 WT β_1-AR outside the 400-nm partition (mean ± S.E.) in ARVMs that were untreated or pretreated with mPKI, or in (C) for cells pretreated with *st*-Ht31 or *st*-Ht31-*pro* is presented. Statistical comparisons were carried out by one-way ANOVA followed by Bonferroni's test. NS, indicates nonsignificant differences between the column pairs or *, **, and *** to indicate $P < 0.05$, $P < 0.01$, and $P < 0.001$, respectively.

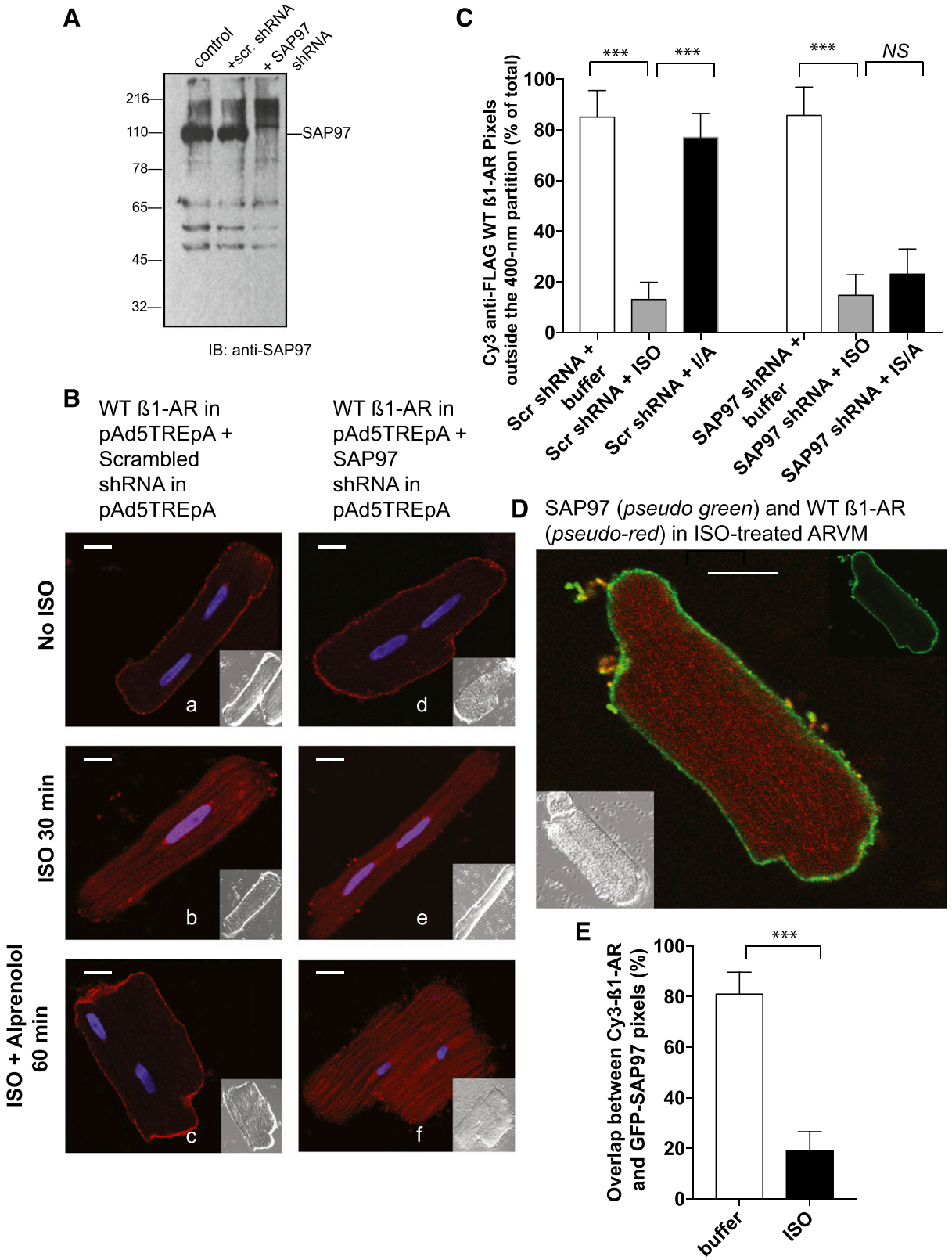

Fig. 5. Characterization of the role and distribution of SAP97 on ISO-mediated translocation of WT β_1-AR in ARVMs. (A) Western blotting of cell lysates (50 μg) prepared from ARVMs that were infected with scrambled Ad-shRNA or Ad-SAP97 shRNA, and then probed with anti-SAP97 IgG. (B) Effect of SAP97 knockdown on WT β_1-AR compartmentalization in ARVMs. ARVMs infected simultaneously with 50 multiplicities of infection (m.o.i.) of Ad-WT FLAG β_1-AR and with either 50 m.o.i. scrambled Ad-shRNA (images a–c) or Ad-SAP97 shRNA (images d–f) were used. These slides were incubated with buffer (images a and d), ISO for 30 minutes (images b and e) or ISO/ALP (images c and f) and processed as described in Fig. 1A. Each scale bar in (B) represents 15 μm. (C) Effect of scrambled vs. SAP97 shRNA on the mean ± S.E. for the distribution of WT β_1-AR pixels outside the 400-nm partition in ARVMs exposed to buffer, ISO, and ISO/ALP is presented. These data were derived from 10 images/condition for three separate experiments, n = 30 images). Statistical comparisons were carried out by one-way ANOVA followed by Bonferroni's test. NS, indicates nonsignificant differences between

hampered by technical hurdles, the chief among them being the low densities of β-ARs in the heart and insufficient sensitivity of currently available antibodies to detect these receptors in intact tissue or ARVMs. We overcame these difficulties by expressing N-terminally FLAG-tagged β_1-AR constructs at relatively low levels and minimized serum-induced cellular differentiation and β_1-AR activation by culturing the ARVMs in serum-free media (Banyasz et al., 2008; Pavlović et al., 2010; Louch et al., 2011). Our results indicate that in quiescent ARVMs, β_1-ARs were localized (>85%) to nontubular external membrane (surface sarcolemma) and to structures around the nucleus that were described previously (Boivin et al., 2006). Activation of the β_1-AR by ISO induced the redistribution of surface β_1-AR into acid and antibody inaccessible vesicles. These findings are significant on several fronts. First, they correlate findings made by other techniques that selective local stimulation of β_1-ARs in the crest region or around T-tubules of ARVMs induced robust widespread activation of cAMP signals, while stimulation of β_2-ARs in T-tubules generated restricted cAMP signals (Nikolaev et al., 2010). Other studies using similar techniques to those described here have shown that β_1-ARs were uniformly distributed at the cell surface membrane and T-tubules, resulting in a striated fluorescence pattern (Zhou et al., 2000). We attribute differences in β_1-AR distribution to the use of fetal bovine serum, which contains catecholamines that can significantly activate β-ARs in some cells lines (Dibner and Insel, 1981; Patrizio et al., 1996) and might alter the cellular distribution of the β_1-AR in naive ARVMs. Finally, we point out that results similar to those described here were obtained by [^{3}H]CGP-12177 binding to cell-surface β-ARs in mouse ventricular myocytes (Cheng et al., 2005). In this study, [3H]CGP-12177 binding was reduced by >60% upon exposing the myocytes to ISO, followed by restoring the density of cell-surface β-ARs by >80%, within 1 hour after ISO washout.

Novel Aspects of β_1-AR Redistribution in ARVMs. Distribution of β_1-ARs in ARVMs under β-agonist activating conditions indicated that β_1-ARs redistributed to small round structures and were no longer exposed to the extracellular milieu. These findings raise a question on the nature of the punctate vesicular structures harboring the β_1-AR in agonist-exposed ARVMs. Our findings indicate that these small diameter vesicles overlapped by >90% with Di-8 ANEPPS staining, a widely used fluorescent dye that specifically labels T-tubules in muscle tissue (Lyon et al., 2009; Pérez-Treviño et al., 2015; Schobesberger et al., 2017). Since T-tubules are continuous with the plasma membrane (Soeller and Cannell, 1999), we did not refer to this process as agonist-mediated internalization of the GPCRs, rather as redistribution/translocation of the GPCRs into T-tubules. We speculate that redistribution of β_1-ARs in ISO-exposed ARVMs into the t-tubular membrane might occur either by vesicular budding (pathways 1 and 2 in Fig. 2A) or translocation of outer membrane structures into T-tubules as illustrated by pathway 3 in Fig. 2A. In this regard, we determined that SNX27 was not colocalized with β_1-AR-containing vesicles in ISO-treated ARVMs (Fig. 2C). This was surprising because SNX27 is an early endosomal PDZ protein that is universally involved in endosome to plasma membrane recycling of PBM-containing cargoes, such as β_1-ARs, β_2-ARs, and many other GPCRs (Lauffer et al., 2010; Steinberg et al., 2013). We interpret this finding as an indication that the agonist-activated β_1-ARs did not migrate into classic endosomes, but might have redistributed to deep invaginations that are continuous with the plasma membrane of cardiac myocytes, such as T-tubules or caveolae (Soeller and Cannell, 1999) (Fig. 2C).

Finally, we determined that ISO washout promoted the translocation of β_1-ARs from these punctate structures back into the plasma membrane, in line with observations concerning the distribution of WT β_1-ARs in other mammalian cells (Gardner et al., 2004; Li et al., 2013; Nooh and Bahouth, 2017). While these results indicate significant similarities in compartmentalization of β_1-ARs in terminally differentiated ARVMs to those in established cell lines (Valentine and Haggie, 2011; Bahouth and Nooh 2017; Nooh and Bahouth, 2017), it also reveals some major differences in redistribution that will be discussed in the subsequent sections.

Role of Barcodes in Setting the Trafficking Itinerary of the β_1-AR in ARVMs. A consistent finding in GPCR trafficking studies is the paramount role of barcodes in dictating the trafficking itineraries of GPCRs. Barcodes are either short amino acid sequences found in the C-tail of the GPCR or reversibly modified amino acids (either by phosphorylation or by ubiquitination), which dictate the trafficking outcome of a given GPCR (Marchese and Trejo, 2013; Bahouth and Nooh, 2017). We concentrated on the roles of the PBM in the C-tail and Ser^{312} in the third intracellular loop in regulating the redistribution of the agonist-activated β_1-AR from intracellular punctate vesicles to the surface membrane of ARVMs because these barcodes were also involved in β_1-AR trafficking in mammalian cells (Gardner et al., 2004, 2007; Nooh et al., 2013; Nooh and Bahouth, 2017). This study confirmed that these domains mediated their effects on the distribution of the WT β_1-AR in ARVMs by a crosstalk mechanism centered around the PBM of the β_1-AR and its binding partner SAP97 (Figs. 4 and 5). Bipartite binding of SAP97 to the PBM of the β_1-AR and to an AKAP5/PKA complex tethered a multi-protein complex to the PBM of the β_1-AR in the surface membrane of quiescent ARVMs (Fig. 6A). Mechanistically, increased cAMP in response to agonist-mediated activation of the β_1-AR activates the pool of PKA bound to the PBM of the β_1-AR to phosphorylate Ser^{312} and other substrates such as L-type Ca^{2+} channels and others (Fig. 6B). In addition, activation of the β_1-AR promotes GRK-mediated phosphorylation of the C-tail of β_1-AR and binding of β-arrestin, which serves as a primary node for GPCR sequestration (Fig. 4B) (Wolfe and Trejo, 2007; Walther and Ferguson,

the column pairs or *, **, and *** to indicate $P < 0.05$, $P < 0.01$, and $P < 0.001$, respectively. (D) Dual-fluorescence confocal microscopy between WT β_1-AR (pseudo red) and SAP97 (pseudo green) in ISO-exposed ARVMs. (E) Statistical comparisons in the percentile of overlapping pixels between the two groups were carried out by student's t test. P values are expressed as NS to indicate no significant difference or *, **, and *** to indicate $P < 0.05$, $P < 0.01$, and $P < 0.001$, respectively.

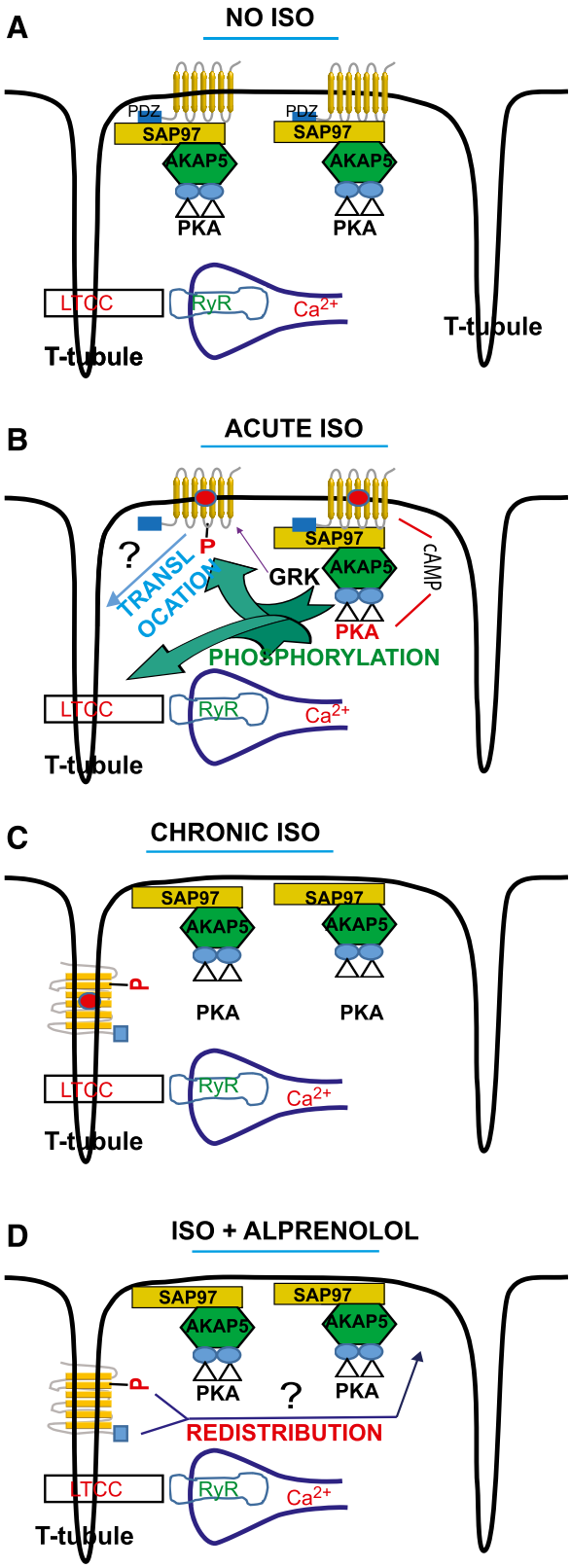

Fig. 6. Effect of ISO on WT β_1-AR compartmentalization in ARVMs. (A) In naive no ISO ARVMs, WT β_1-AR are confined to the surface plasmalemmal membrane. In this compartment, the β_1-AR associates with the PDZ protein SAP97 via its type-1 PDZ. SAP97 in turn binds to the AKAP5/PKA (Gardner et al., 2007) complex. (B) Exposing ARVMs to ISO activated the β_1-AR signaling pathway and increased cAMP, which in turn activated PKA bound to the β_1-AR microdomain. The activated catalytic subunits of PKA phosphorylate many proteins including the β_1-AR on Ser^{312}, L-type calcium channels (LTCCs) and many others. In conditions associated with chronic ISO, the agonist-activated β_1-AR translocated away from the SAP97/AKAP5/PKA complex on the surface membrane to punctate invaginations that appear to correspond to T-tubules by an, as yet, undetermined mechanism. (C) Our results show that under chronic ISO conditions, the β_1-AR resides exclusively in these intracellular structures that overlap with the T-tubule-specific dye Di-8 ANEPPS. (D) Upon replacing ISO with the β-blocker ALP, internal β_1-AR recycled in a type-1 PDZ- and phospho-Ser^{312}-dependent manner from their intracellular compartment to the surface plasmalemmal membrane to restore the organization depicted in the no ISO condition shown in (A). RyR, Ryanodine receptors.

2013). Our findings show that chronic stimulation of ARVMs with ISO induced the redistribution of the majority of WT β_1-AR into punctate structures that overlapped with the structures stained by the T-tubule-specific dye Di-8 ANEPPS (Fig. 2F; Fig. 6C). In this regard, the WT β_1-AR translocated away from the SAP97/AKAP5/PKA complex, which remained in its original compartment at the inner leaflet of the plasma membrane (Fig. 6C). The data in Figs. 3–5 confirm that the type-1 PDZ and its associated receptosome, as well as phospho-Ser^{312}, played a major role in translocating the WT β_1-AR from intracellular structures to the surface plasmalemma of ARVMs (Fig. 6D). This report introduces the (S312A) β_1-AR point mutant as a novel easy-to-use tool for analyzing compartmentalized β_1-AR signaling in intracellular puncta versus the cell surface membrane. These studies would be best carried out by adenoviral-mediated expression of the (S312A) β_1-AR in β_1/β_2-AR knockout mouse cardiomyocytes (Rohrer et al., 1999; Zhou et al., 2000). For example, acute activation of the (S312A) β_1-AR in naive versus ISO-exposed and then rested β_1/β_2-AR$^{-/-}$cardiomyocytes might provide clues regarding the dynamics of β_1-AR signaling to cAMP from the surface membrane or from intracellular structures, respectively, in normal or experimental pathologic conditions.

Summary and Significance of Our Findings in ARVMs. Sustained elevation of circulating catecholamines is a common theme in many pathologic conditions such as cardiac hypertrophy, heart failure, and hypertension (Prichard et al., 1991; Keys and Koch, 2004). In heart failure, increased sympathetic nervous system activity is associated with selective downregulation of cardiac β_1-AR and in worsening prognosis (Bristow et al., 1982; Bristow et al., 1993; Brodde, 1993; Keys and Koch, 2004). In addition, loss or remodeling of T-tubules is a common observation in several cardiovascular diseases such as myocardial infarction and heart failure (Balijepalli et al., 2003; Lyon et al., 2009; Schobesberger et al., 2017). In this report, we show that β-agonists induce the redistribution of the β_1-AR to what appears to be T-tubules or caveolae, which is a novel observation with significant potential for regulating the stability of signaling outputs of cardiac β_1-AR. Whether these combined structural and biochemical abnormalities work cooperatively in altering the compartmentalized signaling outputs or stability of cardiac β_1-AR is not known. However, these changes could provide another investigative dimension for understanding the basis for selective downregulation and desensitization of cardiac β_1-AR seen in heart failure and other pathologic conditions.

Authorship Contributions

Participated in research design: Nooh, Mancarella, Bahouth.

Conducted experiments: Nooh, Mancarella.

Contributed new reagents or analytic tools: Mancarella, Bahouth.

Performed data analysis: Mancarella, Bahouth.

Wrote or contributed to the writing of the manuscript: Nooh, Mancarella, Bahouth.

References

Bahouth SW and Nooh MM (2017) Barcoding of GPCR trafficking and signaling through the various trafficking roadmaps by compartmentalized signaling networks. *Cell Signal* **36**:42–55.

Baig AH, Swords FM, Szaszák M, King PJ, Hunyady L, and Clark AJ (2002) Agonist activated adrenocorticotropin receptor internalizes via a clathrin-mediated G protein receptor kinase dependent mechanism. *Endocr Res* **28**: 281–289.

Baillie GS (2009) Compartmentalized signalling: spatial regulation of cAMP by the action of compartmentalized phosphodiesterases. *FEBS J* **276**: 1790–1799.

Balijepalli RC, Lokuta AJ, Maertz NA, Buck JM, Haworth RA, Valdivia HH, and Kamp TJ (2003) Depletion of T-tubules and specific subcellular changes in sarcolemmal proteins in tachycardia-induced heart failure. *Cardiovasc Res* **59**: 67–77.

Banyasz T, Lozinskiy I, Payne CE, Edelmann S, Norton B, Chen B, Chen-Izu Y, Izu LT, and Balke CW (2008) Transformation of adult rat cardiac myocytes in primary culture. *Exp Physiol* **93**:370–382.

Bers DM (2001) *Excitation–Contraction Coupling and Cardiac Contractile Force*, 2nd ed, Kluwer Academic, Dordrecht, The Netherlands.

Boivin B, Lavoie C, Vaniotis G, Baragli A, Villeneuve LR, Ethier N, Trieu P, Allen BG, and Hébert TE (2006) Functional β-adrenergic receptor signalling on nuclear membranes in adult rat and mouse ventricular cardiomyocytes. *Cardiovasc Res* **71**:69–78.

Bristow MR, Ginsburg R, Minobe W, Cubicciotti RS, Sageman WS, Lurie K, Billingham ME, Harrison DC, and Stinson EB (1982) Decreased catecholamine sensitivity and β-adrenergic-receptor density in failing human hearts. *N Engl J Med* **307**:205–211.

Bristow MR, Minobe WA, Raynolds MV, Port JD, Rasmussen R, Ray PE, and Feldman AM (1993) Reduced β_1 receptor messenger RNA abundance in the failing human heart. *J Clin Invest* **92**:2737–2745.

Brodde OE (1993) Beta-adrenoceptors in cardiac disease. *Pharmacol Ther* **60**: 405–430.

Cheng G, Qiao F, Gallien TN, Kuppuswamy D, and Cooper G, IV (2005) Inhibition of β-adrenergic receptor trafficking in adult cardiocytes by MAP4 decoration of microtubules. *Am J Physiol Heart Circ Physiol* **288**:H1193–H1202.

Delos Santos NM, Gardner LA, White SW, and Bahouth SW (2006) Characterization of the residues in helix 8 of the human β_1-adrenergic receptor that are involved in coupling the receptor to G proteins. *J Biol Chem* **281**: 12896–12907.

Dibner MD and Insel PA (1981) Serum catecholamines desensitize β-adrenergic receptors of cultured C6 glioma cells. *J Biol Chem* **256**:7343–7346.

Ehlers MD (2000) Reinsertion or degradation of AMPA receptors determined by activity-dependent endocytic sorting. *Neuron* **28**:511–525.

Ellisdon AM and Halls ML (2016) Compartmentalization of GPCR signalling controls unique cellular responses. *Biochem Soc Trans* **44**:562–567.

Ferguson SSG, Downey WE, III, Colapietro AM, Barak LS, Ménard L, and Caron MG (1996) Role of β-arrestin in mediating agonist-promoted G protein-coupled receptor internalization. *Science* **271**:363–366.

Fischmeister R, Castro LR, Abi-Gerges A, Rochais F, Jurevicius J, Leroy J, and Vandecasteele G (2006) Compartmentation of cyclic nucleotide signaling in the heart: the role of cyclic nucleotide phosphodiesterases. *Circ Res* **99**: 816–828.

Gardner LA, Delos Santos NM, Matta SG, Whitt MA, and Bahouth SW (2004) Role of the cyclic AMP-dependent protein kinase in homologous resensitization of the β_1-adrenergic receptor. *J Biol Chem* **279**:21135–21143.

Gardner LA, Naren AP, and Bahouth SW (2007) Assembly of an SAP97-AKAP79-cAMP-dependent protein kinase scaffold at the type 1 PSD-95/DLG/ZO1 motif of the human β_1-adrenergic receptor generates a receptosome involved in receptor recycling and networking. *J Biol Chem* **282**:5085–5099.

Gardner LA, Tavalin SJ, Goehring AS, Scott JD, and Bahouth SW (2006) AKAP79-mediated targeting of the cyclic AMP-dependent protein kinase to the β_1-adrenergic receptor promotes recycling and functional resensitization of the receptor. *J Biol Chem* **281**:33537–33553.

Hanyaloglu AC and von Zastrow M (2008) Regulation of GPCRs by endocytic membrane trafficking and its potential implications. *Annu Rev Pharmacol Toxicol* **48**: 537–568.

Head BP, Patel HH, Roth DM, Lai NC, Niesman IR, Farquhar MG, and Insel PA (2005) G-protein-coupled receptor signaling components localize in both sarcolemmal and intracellular caveolin-3-associated microdomains in adult cardiac myocytes. *J Biol Chem* **280**:31036–31044.

Jean-Alphonse F, Bowersox S, Chen S, Beard G, Puthenveedu MA, and Hanyaloglu AC (2014) Spatially restricted G protein-coupled receptor activity via divergent endocytic compartments. *J Biol Chem* **289**:3960–3977.

Keys JR and Koch WJ (2004) The adrenergic pathway and heart failure. *Recent Prog Horm Res* **59**:13–30.

Lauffer BE, Melero C, Temkin P, Lei C, Hong W, Kortemme T, and von Zastrow M (2010) SNX27 mediates PDZ-directed sorting from endosomes to the plasma membrane. *J Cell Biol* **190**:565–574.

Lefkowitz RJ (1998) G protein-coupled receptors. III. New roles for receptor kinases and β-arrestins in receptor signaling and desensitization. *J Biol Chem* **273**: 18677–18680.

Lefkowitz RJ, Rockman HA, and Koch WJ (2000) Catecholamines, cardiac β-adrenergic receptors, and heart failure. *Circulation* **101**:1634–1637.

Li X, Nooh MM, and Bahouth SW (2013) Role of AKAP79/150 protein in β1-adrenergic receptor trafficking and signaling in mammalian cells. *J Biol Chem* **288**:33797–33812.

Louch WE, Sheehan KA, and Wolska BM (2011) Methods in cardiomyocyte isolation, culture, and gene transfer. *J Mol Cell Cardiol* **51**:288–298.

Lyon AR, MacLeod KT, Zhang Y, Garcia E, Kanda GK, Lab MJ, Korchev YE, Harding SE, and Gorelik J (2009) Loss of T-tubules and other changes to surface topography in ventricular myocytes from failing human and rat heart. *Proc Natl Acad Sci USA* **106**:6854–6859.

Marchese A and Trejo J (2013) Ubiquitin-dependent regulation of G protein-coupled receptor trafficking and signaling. *Cell Signal* **25**:707–716.

Morisco C, Zebrowski DC, Vatner DE, Vatner SF, and Sadoshima J (2001) β-adrenergic cardiac hypertrophy is mediated primarily by the β_1-subtype in the rat heart. *J Mol Cell Cardiol* **33**:561–573.

Nikolaev VO, Moshkov A, Lyon AR, Miragoli M, Novak P, Paur H, Lohse MJ, Korchev YE, Harding SE, and Gorelik J (2010) β_2-adrenergic receptor redistribution in heart failure changes cAMP compartmentation. *Science* **327**: 1653–1657.

Nooh MM and Bahouth SW (2017) Two barcodes encoded by the type-1 PDZ and by phospho-Ser^{312} regulate retromer/WASH-mediated sorting of the ß$_1$-adrenergic receptor from endosomes to the plasma membrane. *Cell Signal* **29**: 192–208.

Nooh MM, Chumpia MM, Hamilton TB, and Bahouth SW (2014) Sorting of β_1-adrenergic receptors is mediated by pathways that are either dependent on or independent of type I PDZ, protein kinase A (PKA), and SAP97. *J Biol Chem* **289**: 2277–2294.

Nooh MM, Naren AP, Kim SJ, Xiang YK, and Bahouth SW (2013) SAP97 controls the trafficking and resensitization of the β-$_1$-adrenergic receptor through its PDZ2 and I3 domains. *PLoS One* **8**:e63379.

Patrizio M, Riitano D, Costa T, and Levi G (1996) Selective enhancement by serum factors of cyclic AMP accumulation in rat microglial cultures. *Neurochem Int* **29**: 89–96.

Pavlović D, McLatchie LM, and Shattock MJ (2010) The rate of loss of T-tubules in cultured adult ventricular myocytes is species dependent. *Exp Physiol* **95**: 518–527.

Pelkmans L, Bürli T, Zerial M, and Helenius A (2004) Caveolin-stabilized membrane domains as multifunctional transport and sorting devices in endocytic membrane traffic. *Cell* **118**:767–780.

Pérez-Treviño P, Pérez-Treviño J, Borja-Villa C, García N, and Altamirano J (2015) Changes in T-tubules and sarcoplasmic reticulum in ventricular myocytes in early cardiac hypertrophy in a pressure overload rat model. *Cell Physiol Biochem* **37**: 1329–1344.

Prichard BN, Owens CW, Smith CC, and Walden RJ (1991) Heart and catecholamines. *Acta Cardiol* **46**:309–322.

Rohrer DK, Chruscinski A, Schauble EH, Bernstein D, and Kobilka BK (1999) Cardiovascular and metabolic alterations in mice lacking both β_1- and β_2-adrenergic receptors. *J Biol Chem* **274**:16701–16708.

Romero G, von Zastrow M, and Friedman PA (2011) Role of PDZ proteins in regulating trafficking, signaling, and function of GPCRs: means, motif, and opportunity. *Adv Pharmacol* **62**:279–314.

Schobesberger S, Wright P, Tokar S, Bhargava A, Mansfield C, Glukhov AV, Poulet C, Buzuk A, Monszpart A, Sikkel M, et al. (2017) T-tubule remodelling disturbs localized β_2-adrenergic signalling in rat ventricular myocytes during the progression of heart failure. *Cardiovasc Res* **113**:770–782.

Seaman MN, Gautreau A, and Billadeau DD (2013) Retromer-mediated endosomal protein sorting: all WASHed up! *Trends Cell Biol* **23**:522–528.

Shcherbakova OG, Hurt CM, Xiang Y, Dell'Acqua ML, Zhang Q, Tsien RW, and Kobilka BK (2007) Organization of β-adrenoceptor signaling compartments by sympathetic innervation of cardiac myocytes. *J Cell Biol* **176**:521–533.

Shenoy SK, McDonald PH, Kohout TA, and Lefkowitz RJ (2001) Regulation of receptor fate by ubiquitination of activated β_2-adrenergic receptor and β-arrestin. *Science* **294**:1307–1313.

Simpson DG, Majeski M, Borg TK, and Terracio L (1999) Regulation of cardiac myocyte protein turnover and myofibrillar structure in vitro by specific directions of stretch. *Circ Res* **85**:e59–e69.

Snyder EM, Philpot BD, Huber KM, Dong X, Fallon JR, and Bear MF (2001) Internalization of ionotropic glutamate receptors in response to mGluR activation. *Nat Neurosci* **4**:1079–1085.

Soeller C and Cannell MB (1999) Examination of the transverse tubular system in living cardiac rat myocytes by 2-photon microscopy and digital image-processing techniques. *Circ Res* **84**:266–275.

Steinberg F, Gallon M, Winfield M, Thomas EC, Bell AJ, Heesom KJ, Tavaré JM, and Cullen PJ (2013) A global analysis of SNX27-retromer assembly and cargo specificity reveals a function in glucose and metal ion transport. *Nat Cell Biol* **15**:461–471.

Vaidyanathan R, Taffet SM, Vikstrom KL, and Anumonwo JM (2010) Regulation of cardiac inward rectifier potassium current (I_{K1}) by synapse-associated protein-97. *J Biol Chem* **285**:28000–28009.

Valentine CD and Haggie PM (2011) Confinement of β_1- and β_2-adrenergic receptors in the plasma membrane of cardiomyocyte-like H9c2 cells is mediated by selective interactions with PDZ domain and A-kinase anchoring proteins but not caveolae. *Mol Biol Cell* **22**:2970–2982.

Walther C and Ferguson SS (2013) Arrestins: role in the desensitization, sequestration, and vesicular trafficking of G protein-coupled receptors. *Prog Mol Biol Transl Sci* **118**:93–113.

Wileman T, Harding C, and Stahl P (1985) Receptor-mediated endocytosis. *Biochem J* **232**:1–14.

Wolfe BL and Trejo J (2007) Clathrin-dependent mechanisms of G protein-coupled receptor endocytosis. *Traffic* **8**:462–470.

Xiao RP (2001) β-Adrenergic signaling in the heart: dual coupling of the β_2-adrenergic receptor to G_s and G_i proteins. *Sci STKE* **2001**:re15.

Zhou YY, Yang D, Zhu WZ, Zhang SJ, Wang DJ, Rohrer DK, Devic E, Kobilka BK, Lakatta EG, Cheng H, et al. (2000) Spontaneous activation of β_2- but not β_1-adrenoceptors expressed in cardiac myocytes from $\beta_1\beta_2$ double knockout mice. *Mol Pharmacol* **58**:887–894.

Zhu WZ, Zheng M, Koch WJ, Lefkowitz RJ, Kobilka BK, and Xiao RP (2001) Dual modulation of cell survival and cell death by β_2-adrenergic signaling in adult mouse cardiac myocytes. *Proc Natl Acad Sci USA* **98**:1607–1612.

Address correspondence to: Suleiman W. Bahouth, Department of Pharmacology, The University of Tennessee HSC, 71 S. Manassas, Memphis, TN 38103. E-mail: sbahouth@uthsc.edu